Correlation-Boosted Ensemble Local Patterns for Photoplethysmographic Signal Quality Classification

Giovani Lucafo, Rafael Lima, Italo Sandoval, Luz Albany, and Otavio Penatti

***Abstract*—Photoplethysmography (PPG) is a key component in a myriad of continuous and non-invasive health monitoring solutions, increasingly widespread in wearable devices, such as smartwatches and smart rings. Its high susceptibility to noise, such as motion artifacts and ambient light interference, however, can significantly hinder the learning process, as well as the resulting performance, of the deployed models. Given that, a Signal Quality Assessment (SQA) auxiliary module is usually employed in such applications, for upfront selection of the PPG segments that should be used for reliable extraction of physiological information from the user. Most SQA strategies adopted in these devices rely either on (1) Deep Learning (DL) models, capable of obtaining high performance metrics despite being of increased complexity and energy consumption, or (2) Decision Rule-based strategies that can assess signal quality in an increasedly energy-efficient way, albeit with reduced robustness. In this work, we introduce Hexa-SymmLTP-CC, a novel signal quality classifier composed of an ensemble of Local Pattern-based feature extractors followed by a downstream linear binary classifier, which outperforms state-of-the-art solutions, achieving accuracies of 93.93%, 96.06% and 96.55% across three clinical expert-annotated smartwatch and smart ring PPG datasets, while respecting the lightweight restrictions for wearable-based real-time monitoring applications.**

***Index Terms*—Signal quality assessment, machine learning, local patterns, photoplethysmography, wearable.**

I. Introduction

THE increasingly widespread adoption of wearable devices, such as smartwatches and smart rings, by consumer electronics' users worldwide has prompted a surge of interest in Photoplethysmography (PPG)-based continuous and non-invasive health monitoring solutions. PPG is a widely used cost-effective optical technique for continestimating physiological variables, such as Heart Rate Variability (HRV), Oxygen saturation (SpO_2), Respiratory Rate and Blood Pressure, to name a few. It functions by measuring the changes in absorption of light with known wavelength emmited over the user's skin, mainly in the fingertips and wrists, as a result of the underlying variation in blood volume flow across the different phases of the cardiac cycle.

One of the widely known drawbacks of PPG is its high susceptibility to noise from both motion artifacts [1] and ambient light interference. Those considerably deteriorate PPG morphology, consequently degrading the performance of subsequent feature extraction and inference learning steps on the signal. To overcome such hindrance, an initial Signal Quality Assessment (SQA) module is commonly added to the estimation pipeline, which is in charge of labeling which segments of the incoming PPG are of proper quality for reliable physiological measurements from the aforementioned health applications.

Several approaches have been proposed in the literature for quality assessment of PPG signals, ranging from low-complexity Decision Rule-based strategies [2], [3] to increasingly robust Deep Learning (DL) models [4], [5], [6].

A. Related Work

The work in [5] proposed different DL techniques to assess PPG signal quality, combining one-dimensional data segments with their corresponding two-dimensional projections for subsequent application of image-based classification techniques. Similarly, [7] and [8] proposed PPG quality assessment leveraging 2-D projections with visual transformers (ViT). These two methods also achieved considerable performance, with the same disadvantage of requiring significant computational resources for both model training and prediction.

Authors of [9] presented a hybrid solution based on both time and frequency domain signal representations. Despite the reasonable performance achieved, techniques involving frequency domain required extensive manual tuning in order to better encode the characteristics of the dataset used.

Alternatively, [2] and [3] proposed signal quality assessment using less complex hierarchical decision rules routines, as opposed to DL-based models. Similarly to other works leveraging frequency domain features from the signal, their approaches, despite their effectiveness and reduced computational demands, are highly susceptible to manual adjustments of hyperparameters and thresholds for the decision rules.

Because PPG-based solutions are nowadays widely employed in devices with restricted computational resources, it is often required that the developed signal processing techniques also emphasize lightweight solutions, capable of obtaining a trade-off between performance and low computational cost.

One of the techniques that tackles this trade-off consists of 'Local Binary Patterns' (LBP), which were initially developed to extract image texture features, then later adapted for its application to one-dimensional signals, such as the PPG signal, as in [10]. Such technique focuses on computing a histogram based

Received 4 October 2024; accepted 7 November 2024. Date of publication 11 November 2024; date of current version 16 December 2024. This work was supported by the Samsung Eletrônica da Amazônia Ltda., through the Brazilian Informatics Law 8.248/91. The associate editor coordinating the review of this article and approving it for publication was Dr. Aiping Liu. *(Corresponding author: Rafael Lima.)*

This work involved human subjects or animals in its research. Approval of all ethical and experimental procedures and protocols was granted by the organization "ConseEP Investiga" research institutes under Application No. 074154 and CAAE 07327119.8.0000.5599.

The authors are with the Samsung R&D Institute Brazil, Campinas-SP 13097-104, Brazil (e-mail: g.lucafo@samsung.com; rafael_glima@hotmail.com; italo.sro@samsung.com; l.albany@samsung.com; o.penatti@samsung.com).

Digital Object Identifier 10.1109/LSP.2024.3495573

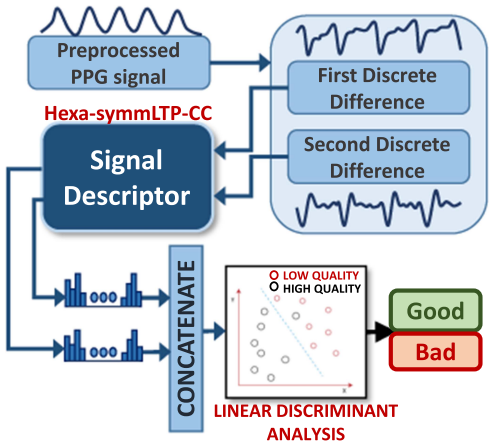

Fig. 1. Overview of the full pipeline of signal quality classification. The first and second discrete difference of the signal are computed from the 3-second PPG window. Then, the Signal Descriptor step extracts histograms as features from the window. Those are subsequently concatenated and fed to a Linear Discriminant Analysis (LDA) binary model that finally outputs the signal quality label.

on the aggregation of binary magnitude comparison information across neighbouring samples throughout the whole extent of the signal. Akin to that, many local pattern techniques and studies have been developed in order to increase the range of applications and the richness of the signal feature extractor. Additionally, [11] proposed a new method of feature extraction based on binary patterns that implemented a hybrid approach merging binary comparisons between samples of the signal itself, which encode morphological information, along with comparisons of statistical attributes from different parts of the signal, such as mean, standard deviation, and median. This added further global information to the histogram locally generated by the binary patterns, improving the overall signal discriminability.

In this work, we propose a novel strategy of generating histograms as one-dimensional signal texture features inspired by the techniques of local patterns. As depicted in Fig. 2, the proposed method consists of a composition of three different feature extraction components that are concatenated to create a combined robust histogram of features. Besides, in addition to substantially improved descriptive properties of the PPG signal, our new method showcases a well-reduced implementation size when compared to DL techniques commonly applied to signal quality classification models, such as Convolutional Neural Networks (CNN) and LSTMs.

In the following, we present all the steps of our new PPG classification pipeline, as well as evidence its advantageous discriminability and compactness properties on experimental results from three different datasets, composed of smartwatch and smart ring PPG signals.

II. Proposed Method

a) Preprocessing: In the present work, we consider the discrete PPG vector $\mathbf{X} = \{x_k\}_0^{N-1} \in \mathbb{R}^N$, sampled with frequency $f_s = 25$ Hz.

The given vector is further windowed into a dataset $\mathcal{X} \in \mathbb{R}^{M \times L}$ of M 3-second non-overlapping samples of length L, in the form

$$\mathcal{X} = \{X_k\}_{k=0}^{M-1}, \text{ with } X_k = \{x_{M \cdot k+j}\}_{j=0}^{L-1} \quad (1)$$

where $L = 3 \cdot f_s = 75$, and $M = \left\lfloor \frac{N}{L} \right\rfloor$.

Additionally, an important step adopted is to use the first discrete difference Δ^1 of the filtered PPG signal and also the second discrete difference Δ^2 (calculated over the first discrete difference):

$$\Delta^1(X_k) = \{X_k[j+1] - X_k[j]\}_{j=0}^{L-2}, \quad (2)$$

$$\Delta^2(X_k) = \{\Delta^1(X_k)[j+1] - \Delta^1(X_k)[j]\}_{j=0}^{L-3}, \quad (3)$$

The calculation of the discrete difference vectors enhances the morphological aspects of the original signal, adding nuances and modifying the way both noisy and regular signals are presented, which adds possible useful information and intensifying noisy behaviors in the signal for better classification of its quality using the descriptors of binary patterns. For the purposes of presenting the proposed model, we will call $W_k = (\Delta^1(X_k), \Delta^2(X_k))$ the tuple composed of the derivatives from 3-second window X_k that will be used as input for the descriptor. This window can be any 1-D signal, however, in our case, it will be both the first and the second discrete derivative of the filtered PPG, as detailed in Fig. 3. As also depicted in Fig. 3, each member of the tuple W window will be further sliced into sub-windows w_i of 8 samples in size with overlap of 1 sample, similarly to the windows of Fig. 2 but without the central element, to be subsequently input to the binary-pattern-based feature extractors.

For a more simplified way of showing the pipeline, W will be used as a generic $(\Delta^1(X_k), \Delta^2(X_k))$ window tuple, and each step will be equally applied to each $\Delta^1(X_k)$ and $\Delta^2(X_k)$ sub-arrays. The model used to receive histograms from the descriptor as input and make binary predictions of signal quality is the Linear Discriminant Analysis model. The full pipeline is shown in Fig. 1.

b) Method Description: The method called Hexa-SymmLTP-CC proposes a hybrid strategy of combining three different feature generation sub-strategies in order to better leverage the descriptive abilities of each one. Each one processes the signal differently, extracting different information about its morphological characteristics and statistical patterns.

Its conceptualization was inspired by binary pattern extraction techniques such as LBP [10] and LTP [12], which differ mainly by the comparison functions Ω_B and Ω_T (see Fig. 2) used to generate binaries.

The LBP-based operator Ω_B, compares two real-valued inputs ($a, b \in \mathbb{R}$) and returns one of the two possibilities (**0** or **1**). The Ω_T, in turn, presents a more generalized comparison than Ω_B, which with the help of the threshold τ, manages to return one of the three possibilities for the comparison of a and b (**0**, **1** and $-$**1**). The threshold τ, here set to $5 \cdot 10^{-3}$, acts as a hyperparameter of the LTP descriptor and can be interpreted as a tolerance variable, responsible for discriminating large differences in signal amplitudes from the milder ones.

In the case of the proposed model, we will refer to each of the three components as Hexa, SymmLTP and CC. The Hexa and SymmLTP components perform the operation of dividing each window W of the signal into sub-windows w_i. This is done due to the fact that they use binary pattern extraction strategies, so each sub-window will generate a decimal to be stored in a histogram, so each of these components will compute a binary pattern for each of the 63 sub-windows, thus generating their own respective histograms, which will be, at the end, concatenated.

A. Hexa Component

Hexa presents a hybrid model inspired by the work of [11] that performs operations on the signal for binary pattern generation

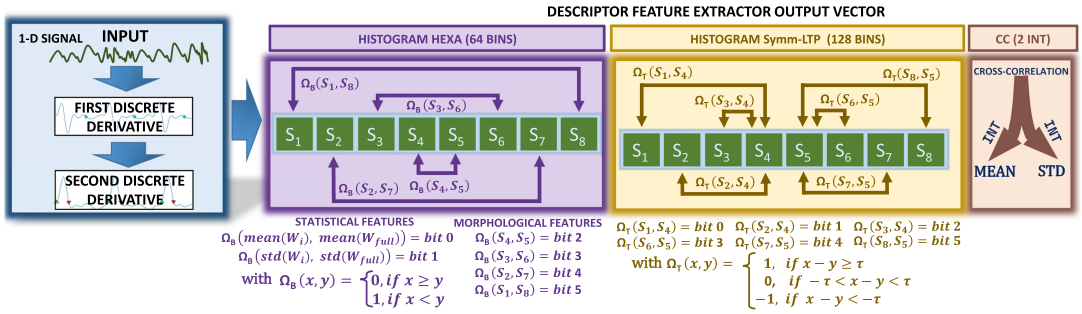

Fig. 2. Visualization of the complete signal feature vector descriptor, which is composed by three sub-descriptors: Hexa, SymmLTP, and CC. The first two are applied to first and second discrete derivatives of each input segment sub-window w_i of size 8 (exemplified by the array of elements S_1 to S_8), and then aggregated across the entire segment. The CC component is computed across the entire segment. The three outputs are further concatenated into a feature vector of size 64 + 128 + 2 = 194, to be fed to a binary classifier, which outputs the corresponding quality label.

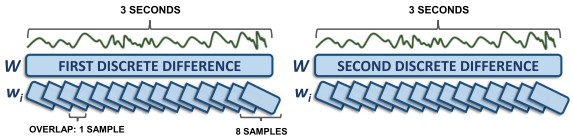

Fig. 3. Visualization of the first and second discrete difference vectors, both 3-second-length derivative windows that are referred as W. Along to each W window is depicted the sub-windows w_i that are 8 samples in size with an overlap of 1 sample, totalling 63 sub-windows for each W PPG window.

using both morphological and signal statistical information. As depicted in Fig. 2, comparisons are made in pairs of samples following the two central samples outwards. Considering the number of neighbors as the number of samples on each side, we have in this case 4 neighbors, thus generating 2^4 possibilities of binaries. In addition to the 4 morphological bits, 2 more statistical bits will be calculated by comparing $\Omega_B(mean(W), mean(w_i))$ and $\Omega_B(std(W), std(w_i))$. Each of these comparisons establishes a relationship between each sub-window and the window W under analysis that will be encoded in the binary along with the morphological information of the signal. At the end of this process, there will be 6 bits that will generate decimal places in a range of $[0, 2^6 - 1]$ to be stored in the histogram.

B. SymmLTP Component

This component, similarly to [12], as the name suggests, performs ternary comparisons symmetrically between the sample pairs in the analyzed window, as shown in Fig. 2.

Similarly to Hexa component, 6 bits are generated for each sub-window w_i analyzed, but in this case, all these bits carry morphological signal information. Overall, SymmLTP descriptor produces two sub-histograms, generated by mapping ternary values to binary ones. The final histogram computed by the SymmLTP component will have a final size of 128, taking into account that the 6 bits of ternary comparisons generate a 64 bins histogram from mapping $-1 \rightarrow 0$ and another 64 bins histogram from mapping $-1 \rightarrow 1$ and $1 \rightarrow 0$.

C. (Auto) Cross Correlation (CC) Component

The third and final component of the model differs from the previous ones in that it does not process the w_i sub-windows. From each entire 3-second PPG window W, the (auto) cross-correlation is computed, extracting further information regarding repetitive patterns of the signal in the window. Its calculation procedure performs a slide of the window on itself, multiplying each element by its correspondent and adding to each iteration. Finally, the value is stored in the final vector C. At the end of the C vector computing, two features are extracted from it, to be concatenated to the previously generated histograms. These features are the mean and standard deviation of C. As these values are floating point type and the histograms generated by the first two components have only integers, a transformation is necessary in order to standardize the feature types. This transformation is done by multiplying the mean and standard deviation of C by 100 and casting to integer. These two features help in the training process by adding valuable information about the signal and not impacting the robustness of the original histograms.

III. Results

In the following, we validate the effectiveness of the proposed ensemble classifier, Hexa-SymmLTP-CC, in three different datasets. All the datasets were fully annotated by clinical experts assisted by an annotation tool, resulting in binary labels for 'good quality' or 'bad quality' for each signal sample. After the dataset windowing, the label for each 3-second segment was given based on the label with most prevalence across its extension.

Our proposed method was compared against three types of state-of-the-art signal classifiers from the literature: 1) DL-based ones, such as in the works of [4]; 2) Local Binary Pattern-based ones [10]; 3) And Decision Rule-based ones [2]. For the purposes of all experiments, the PPG data was first filtered with a 2nd order butterworth bandpass filter from 0.8 to 4.5 Hz. All the methods were trained for 100 epochs and 5 trials, with 20% of the training windows used for validation across each epoch, and the best performing epoch across each trial used for test evaluation.

A. ICON Dataset (Samsung Galaxy Watch Active 2)

The ICON dataset [6] consists of PPG measurements from 56 sessions, lasting approximately 50 minutes each, in which the majority of the participants were older than 60 years, with a mean age of 66 years-old and median age of 70 years-old. 45 sessions were used for training and 11 for testing. Table I shows the performance comparison, in which the metrics for 'RP+ViT' and 'MTF+ViT' were reported as in the original paper [7]. The Hexa-SymmLTP-CC outperforms all other models most metrics. As an exception, Lucafo$_2$ [4] had a higher precision. It is

TABLE I
PERFORMANCE COMPARISON OF THE PROPOSED METHOD AND STATE-OF-THE-ART METHODS IN THE ICON [4] DATASET

Method	Accuracy	Precision	Recall	F1-Score	AUC	Coverage	MCC	Kappa	parameters
$Lucafo_1$ [4]	0.8908	0.9458	0.8941	0.9188	0.8887	0.6565	0.7560	0.7522	338222
LBP [10]	0.8985	0.8993	0.9614	0.9293	0.8584	**0.7423**	0.7550	0.7498	11271
$Lucafo_2$ [4]	0.9363	**0.9514**	0.9574	0.9543	**0.9229**	0.6990	0.8497	0.8492	348462
Hao & Bo [2]	0.7482	0.8810	0.7370	0.8026	0.7554	0.5810	0.4768	0.4626	-
RP+ViT [7]	0.8990	0.9029	0.9507	0.9262	-	-	-	-	-
MTF+ViT [7]	0.9031	0.9408	0.9121	0.9262	-	-	-	-	-
Hexa-SymmLTP-CC (Ours)	**0.9393**	0.9466	**0.9671**	**0.9568**	0.9216	0.7094	**0.8556**	**0.8550**	16551

TABLE II
ABLATION TEST TO VERIFY PERFORMANCE OF DIFFERENT COMBINATIONS OF THE COMPONENTS OF THE PROPOSED METHOD

Method	Accuracy	Precision	Recall	F1	AUC
Hexa	0.9352	0.9406	0.9679	0.9540	0.9145
SymmLTP	0.9182	0.9165	0.9707	0.9428	0.8848
CC	0.8726	0.8805	0.9447	0.9115	0.8268
Hexa - CC	0.9353	0.9414	0.9671	0.9541	0.9151
Hexa - SymmLTP	0.9386	0.9452	0.9676	0.9563	0.9201
SymmLTP - CC	0.9319	0.9290	**0.9765**	0.9522	0.9035
Hexa - SymmLTP - CC	**0.9393**	**0.9466**	0.9671	**0.9568**	**0.9216**

LDA is used as classifier.

TABLE III
PERFORMANCE OF THE HEXA-SYMMLTP-CC DESCRIPTOR ON RING DATASET WHEN COMBINED WITH DIFFERENT CLASSIFIERS

Model	Accuracy	Balanced Accuracy	F1-Score	AUC
Random Forest	0.9476	0.8188	0.9715	0.8188
K-Neighbors	0.9616	0.8640	0.9791	0.8640
AdaBoost	0.9610	0.8693	0.9788	0.8693
Bagging	0.9621	0.9011	0.9793	0.9011
Gradient Boosting	0.9651	0.8912	0.9810	0.8912
Extra Trees	0.9607	0.8568	0.9786	0.8568
LinearDiscriminantAnalysis	0.9655	0.9132	0.9811	0.9132
QuadraticDiscriminantAnalysis	0.9428	0.8641	0.9685	0.8641

important to take into account that the Hexa-SymmLTP-CC also has advantages in terms of model size compared to DL-based solutions due to the advantage of generating histograms as a feature, which resulted in a significantly more compact approach compared to neural networks.

In this work, the full SQA pipeline counts with a Linear Discriminant Analysis (LDA) as a final classifier of histograms, due to its low computational cost and straightforward implementation as well as effectiveness in classification. However, other classifiers were tested for comparison purposes, as shown in Table III, achieving similar accuracies compared to LDA, albeit being of increased complexity/size, such as Gradient Boosting, Bagging and Random Forest, thus being less prioritized in solutions focused on wearable devices with restricted memory and processing resources. In order to gauge the contribution of each component descriptor, an ablation analysis was also performed, and shown in Table II.

It is noticeable that both the Hexa component and SymmLTP have considerable descriptive capacity used separately, as well as combined. The CC component, individually, does not achieve strong performance, but assists on increasing discriminability to the histograms generated, improving the accuracy and precision of the model.

B. GW5 Dataset (Samsung Galaxy Watch 5)

The GW5 Dataset comprises 105 sessions, with approximately 35 minutes of recordings each. The PPG data was collected from individuals with a median age of 38 years and 55/45 (M/F) gender ratio, using Galaxy Watch 5 devices. Overall, 80 sessions were used for training and 25 used for testing. In Table IV, we report the mean classification metrics on the test set, across all trials, for each method. Our proposed model outperforms all counterparts in both Accuracy and F1-Score.

TABLE IV
PERFORMANCE COMPARISON OF THE PROPOSED AND STATE-OF-THE-ART METHODS IN THE GW5 DATASET

Method	Accuracy	Precision	Recall	F1-Score	AUC	Coverage	MCC	Kappa	parameters
$Lucafo_1$ [4]	0.8727	0.9975	0.8631	0.9240	0.9195	0.7913	0.5987	0.5335	338222
LBP [10]	0.9528	0.9553	**0.9950**	0.9747	0.7485	0.9525	0.6536	0.6225	11271
$Lucafo_2$ [4]	0.8779	**0.9990**	0.8673	0.9284	**0.9290**	0.7939	0.5949	0.5256	348462
Hao & Bo [2]	0.7493	0.9247	0.7902	0.8521	0.5512	0.7814	0.0693	0.0600	-
Hexa-SymmLTP-CC (Ours)	**0.9606**	0.9785	**0.9783**	**0.9784**	0.8744	**0.9143**	0.7481	0.7481	16551

TABLE V
PERFORMANCE COMPARISON OF THE PROPOSED AND STATE-OF-THE-ART METHODS IN THE RING DATASET

Method	Accuracy	Precision	Recall	F1-Score	AUC	Coverage	MCC	Kappa	parameters
$Lucafo_1$ [4]	0.9197	**0.9971**	0.9153	0.9544	0.9425	0.8436	0.6663	0.6230	338222
LBP [10]	0.9561	0.9738	**0.9785**	0.9762	0.8398	**0.9235**	0.6975	0.6971	11271
$Lucafo_2$ [4]	0.9430	0.9964	0.9414	0.9681	**0.9513**	0.8683	0.7312	0.7046	348462
Hao & Bo [2]	0.7358	0.9342	0.7666	0.8421	0.5769	0.7541	0.0975	0.0798	-
Hexa-SymmLTP-CC (Ours)	**0.9655**	0.9867	0.9756	**0.9811**	0.9133	0.9086	**0.7826**	**0.7809**	16551

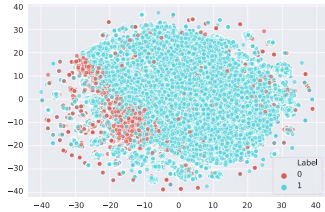

Fig. 4. T-SNE of labelled PPG segments from RING dataset.

TABLE VI
CROSS-TEST PERFORMANCE COMPARISON OF THE PROPOSED AND STATE-OF-THE-ART METHODS IN THE RING DATASET

Method	Accuracy	Precision	Recall	F1-Score	AUC	Coverage	MCC	Kappa	parameters
$Lucafo_1$ [4]	0.0887	0.7500	0.0000	0.0000	0.5000	0.0000	-0.0020	-0.0000	338222
LBP [10]	0.8897	0.9634	0.9136	0.9379	0.7787	0.8641	0.4626	0.4497	11271
$Lucafo_2$ [4]	0.9210	**0.9956**	0.9174	0.9548	**0.9377**	0.8398	**0.6821**	**0.6457**	348462
Hao & Bo [2]	0.0913	0.7380	0.0044	0.0087	0.4942	0.0054	-0.0450	-0.0021	-
Hexa-SymmLTP-CC (Ours)	**0.9265**	0.9786	**0.9399**	**0.9589**	0.8642	**0.8753**	0.6269	0.6157	16551

The models were trained with the ICON dataset.

C. RING Dataset (Samsung Galaxy Ring)

The RING Dataset comprises recordings from 15 sleep sessions amounting to 134 hours of duration in total. The PPG was collected using Samsung Galaxy Ring devices, with 12 sessions were used for training and 3 for testing. As shown in Table V, our proposed model outperforms all counterparts in both Accuracy and F1-Score. Additionally, we computed a T-SNE diagram, depicted in Fig. 4, from which it is possible to assess the overall separability of the ground-truth window labels. Furthermore, the model showcased good performance on transferability of learned parameters: when trained on the ICON dataset and tested on RING data, the model maintained a significant performance, while most other methods had a steep decline in accuracy (see Table VI).

IV. CONCLUSION

The proposed classifier proved to be an effective approach for quality assessment of one-dimensional PPG signals, outperforming a variety of state-of-the-art methods on three different datasets, composed of smartwatch and smart ring sensor data. It is also more compact and efficient than Deep Learning-based techniques, which makes it a compelling PPG signal quality classifier candidate for devices with limited memory and processing resources. One possible limitation of the introduced method is that it was only evaluated with green PPG. Maybe it does not work as effectively for the quality classification of other types of 1-D sensor signals, such as infrared PPG or accelerometer.

REFERENCES

[1] C. Orphanidou, "Quality Assessment for the Photoplethysmogram (PPG)," *Signal Qual. Assessment Physiol. Monitoring: State Art Practical Considerations*, pp. 41–63, 2018.

[2] J. Hao and G. Bo, "A quality assessment system for PPG waveform," in *Proc. IEEE 3rd Int. Conf. Circuits Syst.*, 2021, pp. 170–175.

[3] S. Vadrevu and M. S. Manikandan, "Real-time PPG signal quality assessment system for improving battery life and false alarms," *IEEE Trans. Circuits Syst. II, Exp. Briefs*, vol. 66, no. 11, pp. 1910–1914, Nov. 2019.

[4] G. Lucafo et al., "Signal quality assessment of photoplethysmogram signals using hybrid rule- and learning-based models," *J. Health Informat.*, vol. 15, Jul. 2023.

[5] T. Pereira et al., "Deep learning approaches for plethysmography signal quality assessment in the presence of atrial fibrillation," *Physiol. Meas.*, vol. 40, 2019, Art. no. 125002.

[6] V. B. Fioravanti et al., "Machine learning framework for inter-beat interval estimation using wearable photoplethysmography sensors," *Biomed. Signal Process. Control*, vol. 88, 2024, Art. no. 105689.

[7] P. G. Freitas, R. Lima, G. D. Lucafo, and O. A. B. Penatti, "Photoplethysmogram signal quality assessment via 1D-to-2D projections and vision transformers," in *Proc. IEEE 15th Int. Conf. Qual. Multimedia Experience*, Ghent, Belgium, Jun. 2023, pp. 165–170.

[8] P. G. Freitas, R. G. de Lima, G. D. Lucafo, and O. A. B. Penatti, "Assessing the quality of photoplethysmograms via Gramian angular fields and vision transformer," in *Proc. IEEE 31st Eur. Signal Process. Conf.*, 2023, pp. 1035–1039.

[9] Y. Zhang and J. Pan, "Assessment of photoplethysmogram signal quality based on frequency domain and time series parameters," in *Proc. IEEE 10th Int. Congr. Image Signal Process., BioMed. Eng. Inform.*, 2017, pp. 1–5.

[10] N. Chatlani and J. J. Soraghan, "Local binary patterns for 1-D signal processing," in *Proc. IEEE 18th Eur. Signal Process. Conf.*, 2010, pp. 95–99.

[11] T. Tuncer, S. Dogan, G. Naik, and P. Pławiak, "Epilepsy attacks recognition based on 1D octal pattern, wavelet transform and EEG signals," *Multimedia Tools Appl.*, vol. 80, no. 16, pp. 25197–25218, 2021.

[12] X. Tan and B. Triggs, "Enhanced local texture feature sets for face recognition under difficult lighting conditions," *IEEE Trans. Image Process.*, vol. 19, no. 6, pp. 1635–1650, Jun. 2010.